Epitaxial growth of Fe_3Si/GaAs(001) hybrid structures

Jens Herfort,[a] Hans-Peter Schönherr, and Klaus H. Ploog
Paul-Drude-Institut für Festkörperelektronik, Hausvogteiplatz 5-7, 10117 Berlin, Germany

(Received 5 August 2003; accepted 12 September 2003)

We have established an optimized growth temperature range, namely, 150 °C$<T_G<$250 °C, where ferromagnetic Fe_3Si/GaAs(001) hybrid structures with high crystalline and interfacial quality can be fabricated by molecular-beam epitaxy. The composition of the Fe_3Si layers, which can be regarded as a Heusler alloy, was tuned within the stable Fe_3Si phase. The layers show high magnetic moments with a value of 1050 emu/cm^3, which is close to that of bulk Fe_3Si. © *2003 American Institute of Physics.* [DOI: 10.1063/1.1625426]

Epitaxial ferromagnet/semiconductor (FM/SC) heterostructures have attracted considerable attention due to their possible application in future magnetoelectronics.[1] Most of the work so far has been concentrated on the elements Fe,[2,3] Co,[4] and the binary alloy Fe_xCo_{1-x},[5] which grow epitaxially on GaAs(001) substrates and are ferromagnetic at room temperature. However, the growth temperature has to be kept very low, that is, close to room temperature, to prevent the formation of interfacial compounds at the FM/SC interface, which are detrimental for the realization of spin injection from a FM metal into a SC.[3–6] Nevertheless, using optimized growth conditions of the Fe/GaAs(001) interface, we recently demonstrated spin injection at room temperature, although the spin injection efficiency remained low.[7] Therefore, it is highly desirable to obtain alternative materials that show improved interfacial quality as well as a higher thermal stability of the FM/SC interface.

Surprisingly, only a little work has been done on the growth of Fe_3Si on GaAs(001), despite the fact that it is almost lattice matched to GaAs and is ferromagnetic up to 840 K.[8] Fe_3Si has the cubic DO_3 structure and can be regarded as a Heusler alloy Fe_2FeSi as there are two distinct crystallographic and magnetic Fe sites.[9] Moreover, certain Heusler alloys are predicted to be 100% spin polarized at the Fermi level (i.e., they exhibit half-metallic behavior[10]), hence making Fe_3Si an attractive alternative material for electrical spin injection.

In this report, we present our results on the fabrication and characterization of epitaxial single-crystal Fe_3Si films grown by molecular-beam epitaxy (MBE) on GaAs(001) substrates. As evidenced by double-crystal x-ray diffraction measurements (DCXRD), an optimized growth temperature regime is established in which ferromagnetic Fe_3Si/GaAs(001) layers with high crystalline and interfacial quality can be obtained.

The GaAs templates are prepared in a separate III–V growth chamber using standard GaAs growth techniques. For the Fe_3Si growth, the substrate is then transferred into a As-free metal deposition chamber through UHV. Fe and Si are codeposited from high-temperature effusion cells at growth temperatures varied between 50 and 500 °C, at a growth rate of 0.4 nm/min with a base pressure of 1×10^{-10} Torr. The thickness for all layers is between 30 and 40 nm. The evaporation rates are controlled by the cell temperatures and are adjusted by measuring the beam-equivalent pressure using a Bayard–Alpert ionization gauge. To change the composition, we kept the Fe cell temperature $T_{Fe}=1350$ °C constant, and changed the Si cell temperature T_{Si} in the range between 1360 and 1410 °C. The growth of Fe_3Si is initiated on an As-rich (2×1) reconstructed GaAs(001) surface similar to our previous work[3] on Fe/GaAs(001) in order to avoid the formation of macroscopic defects. The growth was monitored *in situ* using reflection high-energy electron diffraction (RHEED). Immediately upon deposition of about 1 monolayer (ML) Fe_3Si, a sharp, streaky (2×2) RHEED pattern is established that does not significantly change during further growth. After a few monolayers, sharp Kikuchi lines are observed. This is a clear indication of a two-dimensional growth mode and a rather smooth surface of the films. However, the RHEED pattern changes from a $2\times$ to a more complex $5\times$ pattern along the [110] direction for T_{Si} above 1400 °C, indicating the appearance of a different Fe_xSi_y phase.

Figures 1 and 2 show the results of DCXRD measurements on Fe_3Si films having different composition (i.e., different T_{Si}), and grown at different growth temperatures T_G, respectively. The rocking curves are recorded with a wide-open detector and normalized to the symmetric GaAs(004) reflection of the substrate. The second reflection is due to the Fe_3Si layer. For comparison, we have included in Fig. 1 the rocking curve of a pure Fe film grown at 50 °C, which is the optimized T_G for Fe epitaxy on GaAs(001).[3] Three main results can be deduced from Figs. 1 and 2.

First, with increasing T_{Si}, the Fe_3Si peak systematically shifts with respect to the GaAs main peak due to the different composition of the layers. Note that the Fe_3Si phase covers a range from 10 to 26.6 at. % Si.[11] As the Fe/Si ratio is varied around stoichiometry, any excess Fe will substitute into Si lattice sites and vice versa, leading to different lattice constants of the layers.[12] From the peak separation, the perpendicular lattice mismatch $(\Delta a/a)_\perp$ of the layers is determined, and it varies between $+2$ and -0.85% for T_{Si} between 1360 and 1410 °C, respectively. The layers are tetragonally distorted with a parallel lattice mismatch smaller than 0.01%, as evidenced by DCXRD profiles of asymmetric Bragg reflections (not shown here).

[a]Electronic mail: herfort@pdi-berlin.de

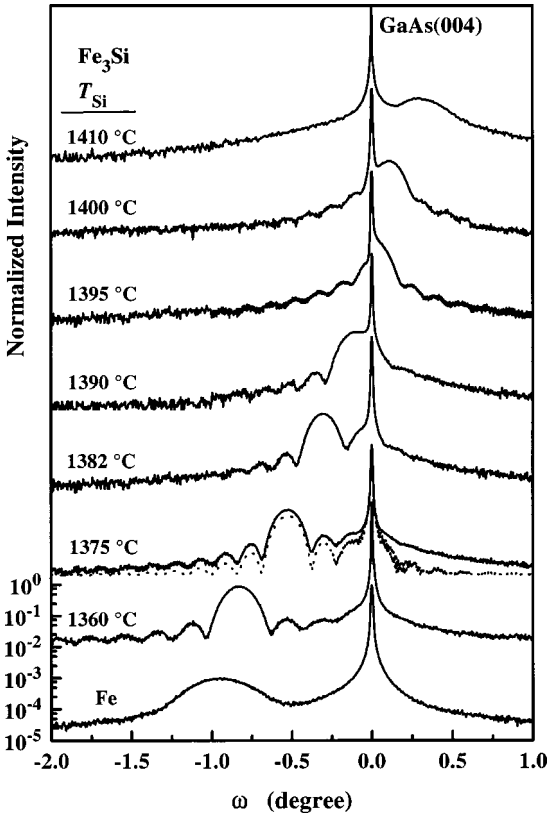

FIG. 1. Semi-logarithmic plots of the normalized intensity of DCXRD rocking curves of various $Fe_3Si/GaAs(001)$ layers grown at 200 °C dependent on the Si cell temperature T_{Si}. The bottom curve belongs to a Fe/GaAs(001) layer grown at 50 °C. The curves are normalized to the GaAs(004) reflection of the substrate. The rocking curves are shifted for clarity. The dotted line shows a simulation for $T_{Si}=1375$ °C.

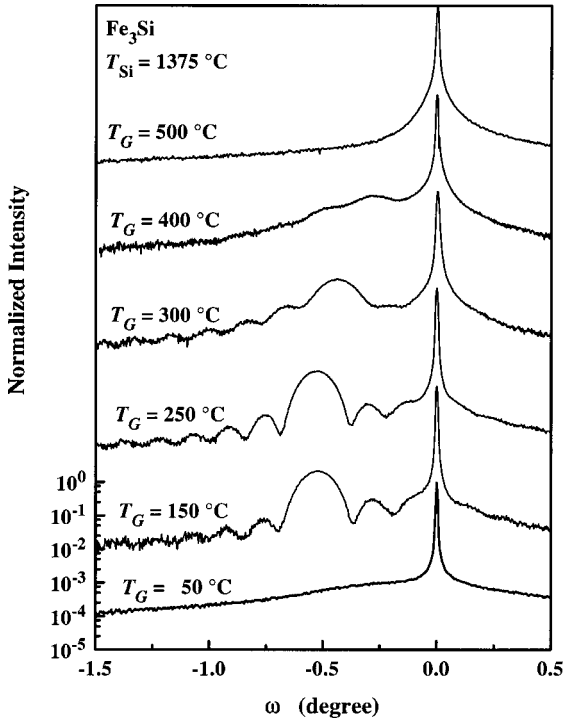

FIG. 2. Semi-logarithmic plots of the normalized intensity of DCXRD rocking curves for various $Fe_3Si/GaAs(001)$ layers grown at a fixed T_{Si} of 1375 °C dependent on the growth temperature T_G. The curves are normalized to the GaAs(004) reflection of the substrate. The rocking curves are shifted for clarity.

Second, both the structural quality and the interface abruptness of the layers first increase with increasing T_{Si} and then decrease above $T_{Si}=1400$ °C. This becomes evident by the appearance of distinct interference (Pendellösung) fringes up to the fifth order and very narrow Fe_3Si peaks. For a qualitative comparison, we have included a simulation of the rocking curve using the Takagi–Taupin formalism for the Fe_3Si layer with $T_{Si}=1375$ °C.[13] Fit parameters are the lattice mismatch $(\Delta a/a)_\perp$ and the layer thickness d, taking into account only the instrumental broadening of the diffractometer. The agreement with the experimental result is excellent, demonstrating high structural perfection as well as abrupt interfaces and very smooth surfaces of the layers. Note that interference fringes were never observed for pure Fe layers, as can be seen in Fig. 1. The full width at half-maximum for the layer with $T_{Si}=1375$ °C is as low as 0.14° compared to 0.39° of a pure Fe layer. The rms surface roughness as determined by atomic force microscopy (AFM) for the layer with $T_{Si}=1375$ °C is 4 Å (taken over 2×2 μm^2). Above $T_{Si}=1400$ °C, the interference fringes disappear and the peaks become much broader, accompanied by larger rms roughnesses $\geqslant$10 Å.

Third, the optimum T_G to obtain single-crystal epitaxial Fe_3Si layers with high structural perfection is found to be between 150 and 250 °C, as can be seen in Fig. 2. For higher T_G, reactions of the Fe and/or Si with the Ga and/or As, similar to that observed for Fe epitaxy on GaAs,[3,6] are very likely to occur. This leads to a gradual disappearance of the Fe_3Si peak, accompanied by a broadening with increasing T_G. Note that for T_G around 500 °C, the growth front is no longer two-dimensional, but exhibits a large number of pyramidal-shaped nanocrystals, as evidenced by AFM. To get further inside any interface reactions and/or structural changes at higher T_G, detailed transmission electron microscopy studies are underway. For lower T_G, the Fe_3Si peak again disappears and only a rather broad profile is obtained, although the surface of the layers remains smooth (rms roughness ~4 Å). This is ascribed to an imperfect substitutional ordering and hence, an inhomogeneous composition of the layer due to the much smaller adatom mobility. It is worthwhile mentioning that the optimum T_G for Fe_3Si is considerably higher than that for Fe, Co, and Fe_xCo_{1-x} on GaAs(001). Hence, Fe_3Si is much more suitable for device processing steps after epitaxial growth, for which temperature cycling well above room temperature is often required.

An accurate determination of the exact stoichiometry of Fe_3Si layers from the DCXRD results is rather difficult due to the rather complex Fe–Si phase diagram and discrepancies in the published data of the relaxed lattice constants a_{Fe_3Si} of the Fe_3Si phase.[8,9,11,14] In Fig. 3, we have plotted a_{Fe_3Si} as a function of the Si content and have summarized results from the literature. In order to get an estimate of the composition of our layers, we have applied the following method. First, we calculated a_{Fe_3Si} using $(\Delta a/a)_\perp$ from the DCXRD rocking curves of Fig. 1, taking into account the elastic constants of Fe_3Si: $C_{11}=219$ GPa and $C_{12}=143$ GPa.[15] We then placed the values of a_{Fe_3Si} on the dashed line, which represents the mean value of the previously published data in the range between 10 and 30 at.% Si. From

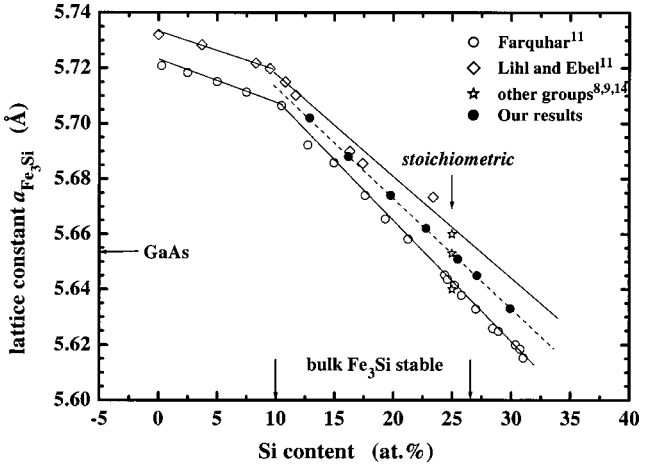

FIG. 3. Dependence of the relaxed lattice constant a_{Fe_3Si} on the Si content for the Fe_3Si phase. The solid lines are guides for the eye. The dashed line gives a mean value in the range of 10 to 30 at. % Si. The solid dots are taken from the results shown in Fig. 1. Note that a larger value of a_{Fe_3Si} belongs to a lower T_{Si} in Fig. 1.

Fig. 3, we can see that the Fe_3Si phase between 10 and 26 at. % Si is correlated with the range of high crystalline and interfacial perfection of the layers in Fig. 1 (namely, for $1360\,°C < T_{Si} < 1395\,°C$), in agreement with the RHEED results mentioned earlier.

The magnetic properties of the layers were measured using superconducting quantum interference device magnetometry at room temperature. Figure 4 shows the magnetization curves of a Fe_3Si layer close to exact stoichiometry, where the magnetic field H is applied in the film plane along the principal crystallographic axes. The layers are ferromagnetic at room temperature, where the easy axis of magnetization is in the film plane along the [100] direction, and the ⟨110⟩ directions are intermediate and slightly nonequivalent. As can be seen in Fig. 4, the magnetic anisotropy is rather small, with coercive fields $H_C \leqslant 1$ Oe (inset of Fig. 4) for all examined orientations. The magnetic moment amounts to 1050 emu/cm^3, which is close to the bulk value of Fe_3Si.[12] A detailed study of the distinct magnetic properties of the layers will be published elsewhere.

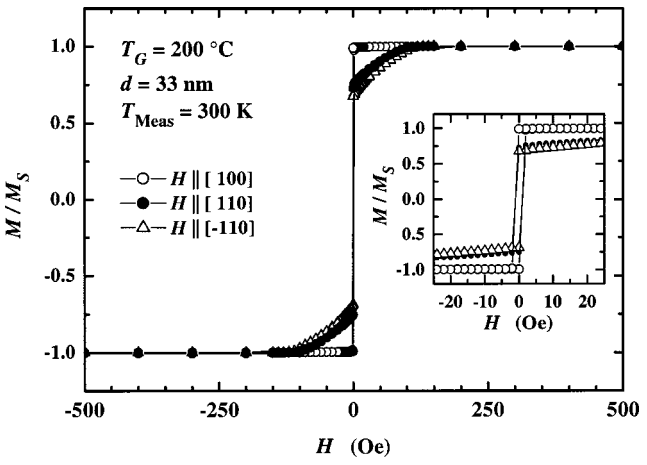

FIG. 4. Hysteresis curves measured at room temperature for a 33 nm Fe_3Si/GaAs(001) layer with the magnetic field H applied in the film plane along various crystallographic orientations. The magnetization M is normalized to the saturation magnetization M_S. The inset shows the hysteresis at very low fields.

In conclusion, we have established an optimized growth temperature range, that is, $150\,°C < T_G < 250\,°C$, in which ferromagnetic Fe_3Si/GaAs(001) hybrid structures with high crystalline and interfacial quality can be fabricated by molecular-beam epitaxy. The results are very promising for the application of Fe_3Si/GaAs(001) hybrid layers for future magnetoelectronics as this system combines high magnetic moments at room temperature with high crystalline and interfacial quality.

This work is partly supported by the German BMBF under contract no. 13N8255. The authors would like to thank O. Brandt for useful discussions.

[1] G. A. Prinz, Phys. Today **48**, 282 (1998).
[2] G. A. Prinz and J. J. Krebs, Appl. Phys. Lett. **39**, 397 (1981); C. Daboo, R. J. Hicken, E. Gu, M. Gester, S. J. Gray, D. E. P. Eley, E. Ahmad, and J. A. C. Bland, J. Appl. Phys. **51**, 15964 (1995); E. M. Kneedler, B. T. Jonker, P. M. Thibado, R. J. Wagner, B. V. Shanabrook, and R. J. Whitman, Phys. Rev. B **56**, 8163 (1997).
[3] H.-P. Schönherr, R. Nötzel, W. Ma, and K. H. Ploog, J. Appl. Phys. **89**, 169 (2001).
[4] K. G. Nath, F. Maeda, S. Suzuki, and Y. Watanabe, J. Appl. Phys. **90**, 1222 (2001).
[5] L. C. Chen, J. W. Dong, B. D. Schulz, B. D. Schultz, C. J. Palmstrom, J. Berezovsky, A. Isakovic, P. A. Crowell, and N. Tabat, J. Vac. Sci. Technol. B **18**, 2057 (2000); M. Dumm, B. Uhl, M. Zölfl, W. Kipferl, and G. Bayreuther, J. Appl. Phys. **91**, 8763 (2002).
[6] A. Fillipe, A. Schuhl, and P. Galtier, Appl. Phys. Lett. **70**, 129 (1997).
[7] H. J. Zhu, M. Ramsteiner, H. Kostial, M. Wassermeier, H.-P. Schönherr, and K. H. Ploog, Phys. Rev. Lett. **87**, 016601 (2001).
[8] M. Hong, H. S. Chen, J. Kwo, A. R. Kortan, J. P. Mannaerts, B. E. Weir, and L. C. Feldman, J. Cryst. Growth **111**, 984 (1991); S. H. Liou, S. S. Malhotra, J. X. Shen, M. Hong, J. Kwo, H. S. Chen, and J. P. Mannaerts, J. Appl. Phys. **73**, 6766 (1993).
[9] P. J. Webster and K. R. A. Ziebeck, *Landolt-Börnstein New Series III/19c* (Springer, Berlin, 1988), p. 104.
[10] R. A. de Groot, F. M. Mueller, P. G. van Engen, and K. H. Buschow, Phys. Rev. Lett. **50**, 2024 (1983); M. J. Otto, H. Feil, R. A. van Bruggen, and C. Haas, J. Magn. Magn. Mater. **70**, 33 (1987); S. Fujii, S. Sugimura, S. Ishida, and S. Asano, J. Phys.: Condens. Matter **43**, 8583 (1990).
[11] For the Fe–Si phase diagram, see M. Hansen, *Constitution of Binary Alloys* (McGraw-Hill, New York, 1958); R. P. Elliot, *Constitution of Binary Alloys, Suppl. 1* (McGraw-Hill, New York, 1965).
[12] W. A. Hines, A. H. Menotti, J. I. Budnick, T. Litrenta, V. Niculescu, and K. Raj, Phys. Rev. B **13**, 4060 (1976).
[13] O. Brandt, P. Waltereit, and K. H. Ploog, J. Phys. D **35**, 577 (2002).
[14] M. Fanciulli, G. Weber, H. van Känel, and N. Onda, Phys. Scr., T **54**, 16 (1994).
[15] G. Kötter, K. Nembach, F. Wallow, and E. Nembach, Mater. Sci. Eng., A **114**, 29 (1989).